

## EXPERIMENTAL STUDY ON GRAPHENE/TRANSITION METAL CHALCOGENIDE BASED ENERGY STORAGE AND CONVERSION

L. ARULMURUGAN<sup>a,\*</sup>, M. ILANKUMARAN<sup>b</sup>,

<sup>a</sup>*Department of Electronics and Communication Engineering,  
Bannari Amman Institute of Technology, Sathyamangalam, Erode, Tamilnadu,  
India*

<sup>b</sup>*Department of Mechatronics Engineering, K S Rangasamy College of Technology,  
Tiruchengode, Tamilnadu, India*

The ever-increasing energy demand and the shortage of fossil fuels force the researchers to do research on utilization and conversion of renewable energy sources. In Recent years, the graphene and Transition Metal Chalcogenide (TMC) based Phase Change material (PCM) have been reviewed towards the future energy storage and energy conversion. This PCM is considered as a promising pathway to alleviate the energy crisis. The TMC material is considered as an emerging material due to their optoelectronic behavior and stability of the material. Moreover, the integration of TMC with graphene, significantly improve the performance of the system. The storage of solar energy in the form of sensible and latent heat has become an important aspect of energy management. To improve the performance of domestic solar water heater system, the vertical spiral and cylindrical heat exchanger is designed. The spiral module and cylindrical modules filled with and without PCM are analyzed and the obtained results are compared with each other. The results show that the spiral and cylindrical heat exchanger filled with PCM store and release the thermal energy efficiently and it performs the desired functions than the without PCM module.

(Received April 28, 2020; Accepted July 14, 2020)

*Keywords:* Graphene/transition metal chalcogenide, Phase change material,  
Thermal management, Heat exchanger, Spiral and cylindrical module

### 1. Introduction

The transition metal chalcogenides are a promising and are now gaining increasing attention for energy applications. The Graphene related two-dimensional crystals and hybrid systems are used for energy conversion and storage applications. The integration of graphene with chalcogenide material offers opportunities to tackle challenges driven by the increasing global energy demand [1]. The chalcogenide material has received tremendous attention in recent years, due to its electrical properties and unique structure of the material. The chalcogenide material shown a potential material for most applications, preferably energy storage and conversion [2]. The global energy crisis and environmental pollution have resulted in an increase in research efforts to develop renewable energy devices. Transition metal chalcogenides have been attracting increasing attentions because of its unique crystal structures and rich physiochemical properties [3]. The ever-increasing energy demands on advanced materials are strongly requested for the exploration of advanced energy storage and conversion technologies. Moreover, the integration of TMCs with conductive graphene host has enabled the significant improvement of electrochemical performance of devices [4]. The transition metal chalcogenides have recently been in the spotlight due to their optoelectronic properties that render them potential candidates mainly in energy conversion applications. Integration of TMCs onto a strong electron- accepting material, such as graphene, yielding novel TMC/graphene ensembles is of high significance [5]. The discovery of graphene marks a major event in the physics and chemistry of materials. The amazing properties of this two-dimensional material have prompted research on other layered materials, of which

---

\* Corresponding author: arulmurugan83@gmail.com

layered transition metal dichalcogenides are important members [6]. Last two decades, PCM have attracted attention in thermal energy storage system. Solar water heater is getting popularity since they are relatively inexpensive and simple to fabricate and maintain. Solar energy applications require a large energy storage capacity in order to cover a demand on minimum number of days in a year. This is commonly achieved by latent heat storage in large water tanks, in which thermal energy is stored as latent heat in substances undergoing a phase transition, e.g., the heat of fusion in the solid–liquid transition. Storage by causing a material to rise in temperature is called sensible heat storage. Storage by phase change, the transition from solid to liquid or from liquid to vapour is another mode of thermal storage known as latent heat storage in which no temperature change is involved. It is possible for both sensible and latent heat storage to occur in same material as when solid is heated, then melted, then raised further in temperature.

The device performances of graphene and chalcogenides based materials are compared with their performance. The unstable nature of phosphorene under ambient condition is discussed along with the various approaches to avoid ambient degradation [7]. The graphene and transition metal chalcogenides are among the most studied ultrathin materials and it is suitable for energy application [8]. The remarkable properties of graphene have renewed interest in inorganic, two-dimensional materials with unique electronic and optical attributes. Transition metal dichalcogenides are layered materials with strong in-plane bonding and weak out-of-plane interactions enabling exfoliation into two-dimensional layers of single unit cell thickness [9]. The graphene based phase change composites are mostly used for thermal management problem in electronics cooling system. The phase change composites prepared by integrating graphene and the phase change material gives a strong iconicity they may exhibit unique physical properties which is beneficial for energy harvesting and other optoelectronic applications [10]. The fabrication of transition metal selenides and their applications in energy storage are summarized systematically and relationship between nanostructures and preparation methods was discussed. The applications of transition metal selenides in energy storage are reviewed and their relationship between nanostructures and electrochemical performance is discussed [11-18]. The recent progress in 2D materials beyond graphene and includes mainly transition metal dichalcogenides are finding niche applications for next-generation electronics and optoelectronics devices. The several challenges in developing scalable and defect-free transition metal dichalcogenides on desired substrates, new growth techniques compatible with traditional and unconventional substrates have been developed to meet the ever-increasing demand of high quality and controllability for practical applications [19]. The proposed method is to reduce the thermal discomfort by using phase change material (PCM) to absorb and to store the excessive heat produced by the solar radiation to attain the comfort cooling for the wearer [20]. The aforementioned literature revealed that the unique properties of graphene and TCM material based phase change material is need an attention for future energy application.

## **2. Materials and methods**

The graphene solution is prepared and mixed with Transition Metal Chalcogenide using the magnetic stirrer method and their characteristics are studied.

### **2.1. Materials**

The graphene material is prepared using Magnetic stirrer method; precursor 0.3g of graphene powder is dissolved in 30ml of ethanol ( $C_2H_5OH$ , 99 %, Scientific and Chemical Suppliers, Erode, India). The precursor solution was put into the magnetic stirrer for about 30 minutes. The prepared graphene solution was mixed with Transition Metal Chalcogenide (barium sulfide powder (Sigma-Aldrich, 99.9%)) under mechanical agitation. The experiment was carried out under normal room temperature for avoiding the potential oxidation of the material.

## 2.2. Preparation of Composite PCM

The PCM composites were prepared by using melting dispersion method. Pure erythritol was weighed and poured into a beaker. Then, it was heated to 120°C to reach the molten state. The graphene solution with mass ratios of 5 wt%, 10 wt%, 15 wt% and 20 wt% were dispersed into separate samples of the liquid PCM and then each one was stirred at 800 rpm with an agitator under room temperature. The magnetic stirrer employs a spinning magnetic field to stir the bar engrossed in a liquid to spin very hastily. A rotating magnetic field is created by a rotating magnet placed beneath the vessel with the liquid. Most chemical reaction takes place in glass vessels as there is no substantial influence of magnetic field over glass. Magnetic stir bars function well inside glass vessels as it is transparent to magnetism. In order to ensure the complete dispersion of PCM composite an ultrasonic generator was employed.

## 2.3. Characterization of Composite PCM

The Differential Scanning Calorimeter (DSC 6000 – Perkin Elmer) was used to measure the solid–liquid phase change temperatures and latent heat capacities of the samples and it is shown in Table 1. The instrument was calibrated with an indium standard. The resolution of DSC is 0.02  $\mu$ W. Five different mixtures of samples were taken for a DSC analysis at a heating rate of 10°C /min in the temperature range of 0~200°C. All these operations were carried out in nitrogen atmosphere.

Table 1. DSC Analysis of Graphene/Transition Metal Chalcogenide.

Sample (%)	Melting Temperature (°C)	Specific Heat (J/g.°C)	Thermal Conductivity (W/mK)	Latent Heat (J/g)
Pure	122.2	2.14	0.754	223.07
5	120.5	2.01	0.831	212.12
10	117.3	1.92	1.174	194.30
15	112.4	1.85	1.231	188.67
20	105.2	1.72	1.423	170.58

The obtained results show that the increasing volume of graphene additives in the TMC material increases the thermal conductivity of the material. The thermal conductivity of graphene is 1.423 W/mK which is twice larger than 20% of graphene/TMC combined PCM (0.754 W/mK). The latent heat of PCM composites decreased from 223.07 J/g to 170.58J/g and melting point of PCM composite decreased from 122.2°C to 105.2°C.

## 3. Experimental study

The solar water tank is used to store the water which is to be heated and the water is recirculated in the solar panel. It is cylinder in shape and made of aluminium (Al) material. It has four openings, two for filling and draining of the water and the other two for circulation of the filled water into the solar panel. Moreover, the top of the solar water is covered by a cap made up of Al, which has provision to hang the PCM modules in the water tank. A stand is used for placing the tank. The front view of solar water tank is shown in figure 1. The tank is placed above the stand in order to provide some pressure to the water to circular into the solar panel. Its storage is about 78 liters.

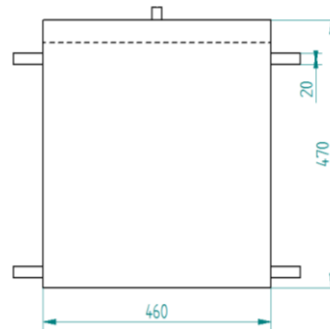


Fig. 1. Front View of Solar Water Tank, all dimensions are in mm.

### 3.1. Cylindrical and spiral pcm module

The front view and top view of cylindrical module is shown in Figs. 2 and 3. Cylindrical PCM module is a thermal energy storage system in the form of cylinder. This module consists of an opening for filling the PCM (Graphene/TMC) inside it, which stores the thermal energy. It is also provided an opening for the insertion of thermocouple. An adjusting threaded rod is also provided for the purpose of hanging inside the water tank. The front view and top view of spiral module is shown in Figs. 4 and 5.

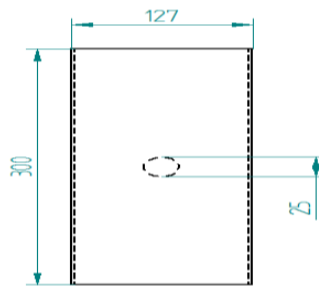


Fig. 2. Front View of Cylindrical Module.

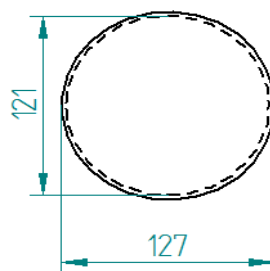


Fig. 3. Top View of Cylindrical Module, all dimensions are in mm.

#### 3.1.1. Specification of cylinder

Material	= Aluminium
Volume of cylinder	= 0.00295 m <sup>3</sup>
Length of cylinder	= 0.3 m
Diameter	= 0.112 m
Inner diameter of cylinder	= 0.121 m
Thickness of cylinder	= 0.003 m

### 3.2. Spiral pcm module

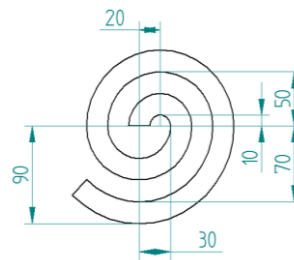


Fig. 4. Top View of Spiral Module

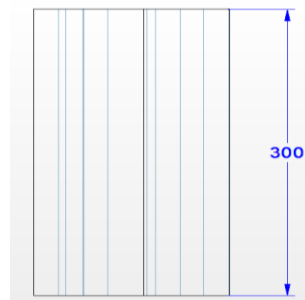


Fig. 5 Front View of Spiral Module, all dimensions are in mm.

### 3.2.1. Specification of spiral pcm module

Material	= Aluminium
Volume of the spiral storage system	= $3.27 \cdot 10^{-3} \text{ m}^3$
Surface area of spiral storage system	= $348507.35 \text{ mm}^2$
Height of the spiral	= 300 mm
Thickness of Al sheet	= 0.8 mm

### 3.2.2. Specification of data logger:

Range	= 0-1200°C
Temperature	= $25^\circ\text{C} \pm 5\%$
Humidity	= 30-65% RH
Accuracy	= $\pm 1^\circ\text{C}$
Type of thermocouple used	= K-type

### 3.2.3. Specifications of thermocouple

Thermocouple type	= K-type
Thermocouple materials	= Alumel-Chromel wire
Probe diameter	= 3 mm
Wire length	= 2.5 m
Maximum temperature	= $150^\circ\text{C}$

## 3.3. Working principle

The schematic diagram and the experimental setup is shown in Figs. 6 and 7 respectively. The inlet and out let pipes are cut to the required length. In order to measure the mass flow rate of the inlet hot water which flows to the tank, a flow meter is fitted to the inlet pipe. To stop water flow between the tank and collector, a ball valve is also fitted to it. Then the pipes are connected and ensured that there is no leakage and water is filled in the storage water tank. The thermocouple and the PCM module are arranged and fitted in the tank's cap and then the tank is closed. The power supply is provided for the data logger and the pen drive is inserted for the purpose of data

storage and the time interval is set as 30min. Initially charging process occurs and then followed by discharging.

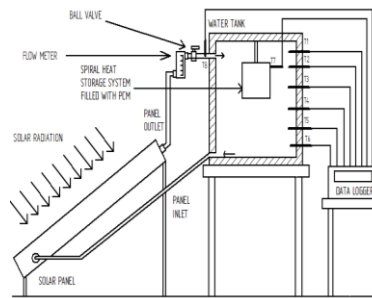


Fig. 6. Schematic View of the Experimental Setup.



Fig. 7. Experimental setup.

The storage unit (packed bed), is a cylindrical storage tank filled with spherical capsules containing a PCM. During discharging, the heat transfer fluid (water) flows over the packed bed from the bottom to the top, and the PCM in the spherical capsules solidifies. The figure 8 shows a schematic diagram of spherical capsule PCM.

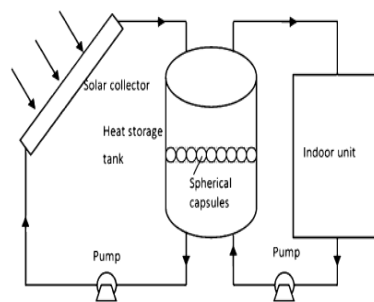


Fig. 8. Schematic Diagram of Spherical Capsule PCM.

The Fig. 9 displays the variation of the temperatures of PCM and HTF with time at different positions. It is clearly seen that the PCM undergoes three stages during the discharging process, such as liquid sensible heat release, solidifying latent heat release and solid sensible heat release.

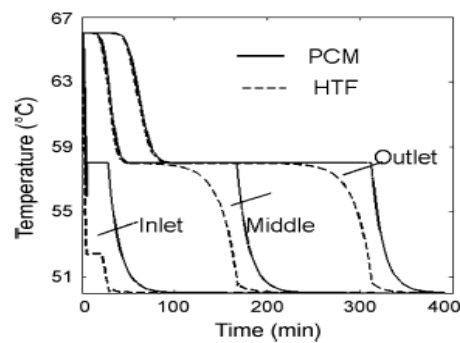


Fig. 9. Variations of the Temperatures of PCM and HTF with Time.

The PCM temperature decreases rapidly at the liquid sensible heat release stage, then it remains uniform at the solidification temperature until the solidification stage terminates. The heat transfer rate decreases as the temperature difference between PCM and HTF decreases along the direction of HTF flow. Hence, it is clear that the closer to the outlet location, the longer time for complete solidification and heat release process.

The inlet temperature and mass flow rate have strong influences on the heat release rate and complete solidification time. The higher flow rate of HTF, the higher heat released rate, and also the less time for complete solidification. The latent efficiency is higher for the higher inlet temperature of HTF than that for the lower inlet temperature of HTF. The higher HTF inlet temperature also results in the lower heat release rate and the longer time for complete solidification. The packed bed initial temperature has a significant effect on latent efficiency, while it has no significant effect on solidification time and heat release rate. The higher initial temperature is not suitable for this solar heat storage system.



Fig. 10. Solar water tank.



Fig. 11. Cylindrical module.



Fig. 12. Spiral module.

During charging process, the cold water which is initially present in the tank enters into the solar flat plate collector. By means of the solar energy which is available during the day time, the collector heats the cold water. As a result of which the water gets heated and is allowed to enter the solar tank through inlet pipe thermosyphonly. The PCM placed in the water tank by means of spiral/cylindrical modules gets heated. As this continues, the temperature increases. When the temperature goes above the melting point of the PCM, phase change occurs (solid to liquid state) and thereby stores the heat energy by means of latent heat storage.

After an average temperature of 70°C is achieved in the water which is stored in the tank, the solar flat plate collector panel is closed and the ball valve is also closed to stop the flow of water from the solar panel to the tank. Now in the tank the water temperature decreases and so the PCM releases the heat energy stored in it and it starts to solidify. The heat energy released by the PCM is absorbed by the water in solar tank. By this way of latent heat storage method, hot water is got for an extended period during night times. This discharging process is carried out till an average temperature of 45°C is achieved in the water present in the solar tank.

These experiments are carried out without the presence of PCM module, with cylindrical PCM module and with spiral PCM modules and the charging time, discharging time and charging energy efficiencies are calculated and compared with each other.

### 3.4. Design and calculation

The dimension of the spiral and cylindrical module are taken from the commercially available heat exchanger. All the module dimensions are taken as millimeter (mm). The calculation of volume, surface area, efficiency, stratification number as given below.

#### 3.4.1. Calculations for spiral module

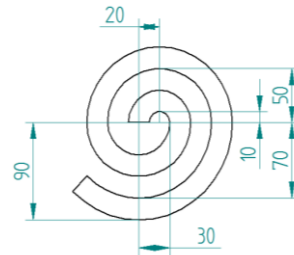


Fig. 13. Dimensions of Spiral Module, all dimensions are in mm

Distance between 2 centers	= 20 mm
Height of spiral storage unit	= 300 mm
Gap between inner and outer spiral	= 20 mm
For outer spiral, radius of 1 <sup>st</sup> curve	= 30 mm
For outer spiral,	
Radius of 2 <sup>nd</sup> curve	= (Radius of 1 <sup>st</sup> Curve + Center Distance)
	= (30+20)
	= 50 mm
Therefore,	
Radius of 3 <sup>rd</sup> curve	= 70 mm
Radius of 4 <sup>th</sup> curve	= 90 mm
For inner spiral,	
Radius of 1 <sup>st</sup> curve	= 10 mm
Radius of 2 <sup>nd</sup> curve	= 30 mm
Radius of 3 <sup>rd</sup> curve	= 50 mm
Radius of 4 <sup>th</sup> curve	= 70 mm

#### 3.4.2. Calculation of volume

Volume of hollow cylinder	$= \frac{\pi}{4} h (D^2 - d^2)$
Volume of hollow semi cylinder 1	$= \frac{\pi}{8} h (D^2 - d^2)$
	$= \frac{\pi}{8} 300 (60^2 - 20^2)$
	$= 376991.11 \text{ mm}^3$
Volume of hollow semi cylinder 2	$= 753982.23 \text{ mm}^3$
Volume of hollow semi cylinder 3	$= 1130973.35 \text{ mm}^3$
Volume of hollow semi cylinder 4 (120°)	$= 1005309.64 \text{ mm}^3$
Therefore,	
Total volume of the spiral storage unit	$= 3267256.33 \text{ mm}^3$
	$= 3.27 \times 10^{-3} \text{ m}^3$

### 3.4.3. Calculation of surface area

$$\begin{aligned}
 \text{Surface area of hollow cylinder} &= 2\pi (R+r) (R-r+h) \\
 \text{Surface area of hollow semi cylinder 1} &= \pi (30+10) (30-10+300) \\
 &= 40212.39 \text{ mm}^2 \\
 \text{Surface area of hollow semi cylinder 2} &= 80424.78 \text{ mm}^2 \\
 \text{Surface area of hollow semi cylinder 3} &= 120637.16 \text{ mm}^2 \\
 \text{Surface area of hollow cylinder 4 (120}^\circ) &= 107233.02 \text{ mm}^2 \\
 \text{Therefore,} & \\
 \text{Total surface area of spiral storage unit} &= 348507.35 \text{ mm}^2
 \end{aligned}$$

### 3.4.4. Calculation for cylindrical pcm module

$$\begin{aligned}
 \text{Volume of cylindrical PCM module, V} &= \frac{\pi}{4} D^2 H \\
 \text{The length of cylinder is fixed, H} &= 0.3 \text{ m}
 \end{aligned}$$

### 3.4.5. Efficiency

$$\eta_{ch} = \frac{T_{avg} - T_{initial}}{T_{inlet} - T_{initial}}$$

Where,

$$\begin{aligned}
 T_{avg} &= \text{Average charging temperature (}^\circ\text{C)} \\
 T_{initial} &= \text{Average initial temperature (}^\circ\text{C)} \\
 T_{inlet} &= \text{Inlet temperature of water (}^\circ\text{C)}
 \end{aligned}$$

### 3.4.6. Stratification Number

$$\begin{aligned}
 \text{Stratification number} &= \frac{\left(\frac{\partial T}{\partial Z}\right)_{t=j}}{\left(\frac{\partial T}{\partial Z}\right)_{t=0}} \\
 \frac{\partial T}{\partial Z} &= \frac{1}{j-1} \left[ \sum_{j=1}^{j-1} \left( \frac{T_j - T_{j+1}}{\Delta Z} \right) \right]
 \end{aligned}$$

Where,

$$\begin{aligned}
 \Delta Z &= \text{Distance between two thermocouples in m} \\
 j &= \text{number of thermocouples.} \\
 T &= \text{temperature in } ^\circ\text{C}
 \end{aligned}$$

## 4. Results and discussion

The Structural characterization was studied by using X-ray diffraction (XRD) method. The studies were performed on the three different mixture of graphene with TMC material (5%, 10% and 20% graphene mixed with TMC material) is shown in figure 14, 15 and 16 respectively. The XRD scans were carried out in a Power X-ray diffractometer, Rigaku corporation, International marketing division, Ultima III Max, Japan. All the samples are rotated at 0.16rps. The integration time of 0.25s and step angle of 0.015° were taken and the spectra were acquired with 2θ range from 10° to 75°. The peak signal represents the mixture of samples graphene and TCM material.

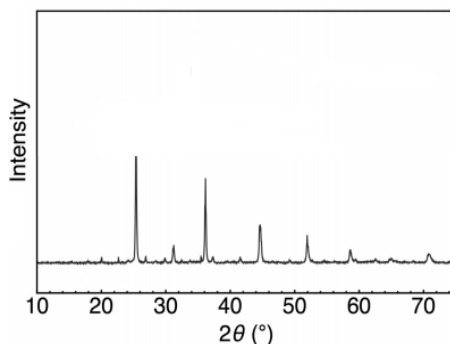


Fig. 14. XRD scans of 5% mixture of graphene with TCM material.

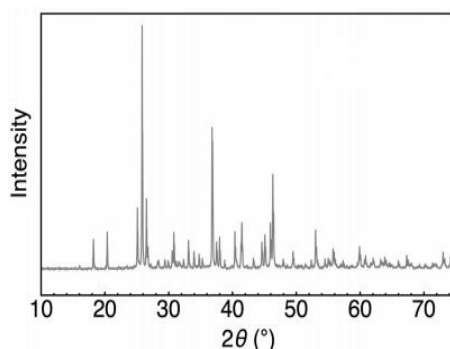


Fig. 15. XRD scan of 10% mixture of graphene with TCM material.

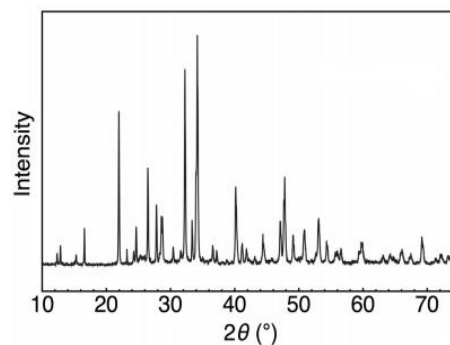


Fig. 16. XRD scan of 20% mixture of graphene with TCM material.

The Raman spectroscopy measurements were performed by using confocal Raman Microscope. It is a High Resolution Micro-Raman spectrometer manufactured by Renishaw, UK. The laser range of spectrometer is 532 nm wide with clear view of 20x based objective lens. The studies were performed on the two different mixture of samples (10% and 20% of graphene mixed with TMC material) is shown in Figs. 17 and 18 respectively. The large peak represents the proper of mixture of samples. The small hikes represent the partial mixture of the samples. The randomly distributed samples are represented in the remaining signal.

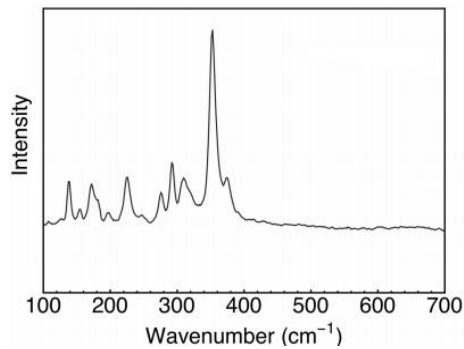


Fig. 17. Raman Spectra of 20% mixture of graphene with TCM material.

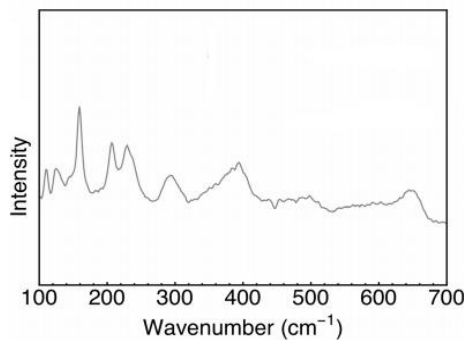


Fig. 18. Raman Spectra of 10% mixture of graphene with TCM material.

The charging discharging of cylindrical and spiral module with heat exchanger was studied and plotted in Figs. 19 to 28. The comparison of PCM with and without the module was investigated and plotted. The thermocouple  $T_1$ ,  $T_2$ ,  $T_3$ ,  $T_4$ ,  $T_5$ ,  $T_6$  are placed in a solar water tank with an equal distance. During the charging period the PCM based module are capable of storing a large amount of heat storage unit and the discharging period the PCM based module are withstanding the heat with a considerable amount of time. The obtained result shows that the PCM based modules are efficiently storing and releasing the heat in the form melting and solidification. The below graph compares PCM temperature with time during discharge of spiral module.

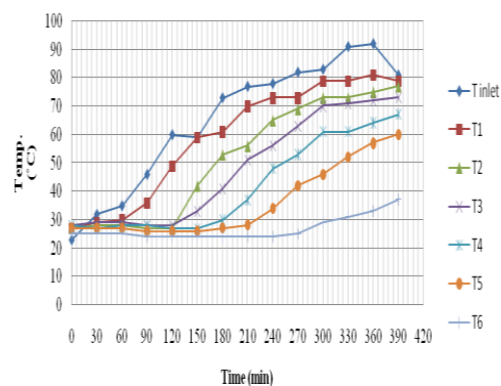


Fig. 19. Charging Without PCM.

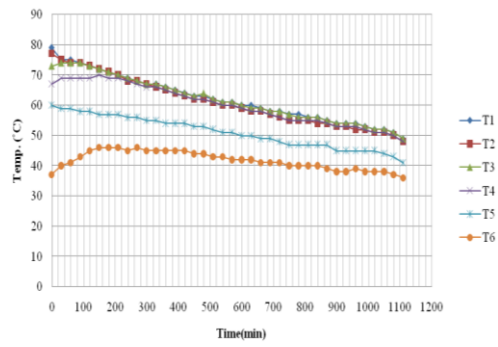


Fig. 20. Discharging without PCM Module.

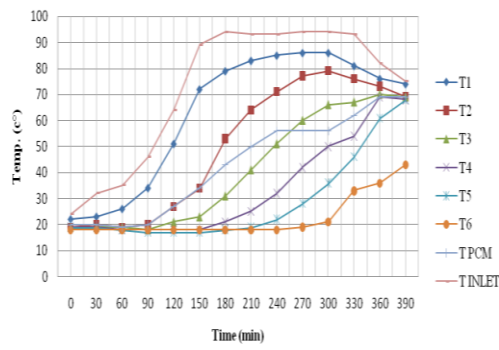


Fig. 21. Charging with Cylindrical PCM Module.

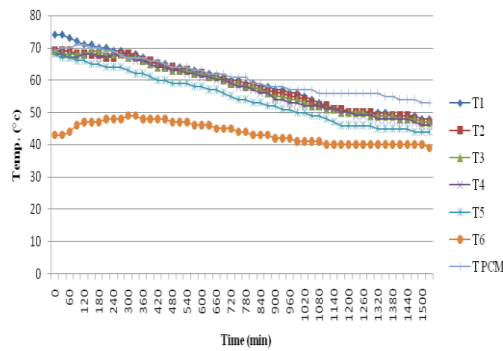


Fig. 22. Discharging with Cylindrical PCM Module.

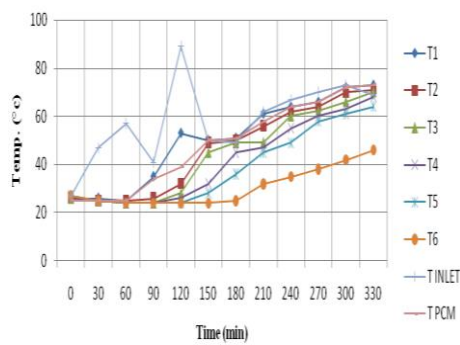


Fig. 23. Charging with Spiral PCM Module.

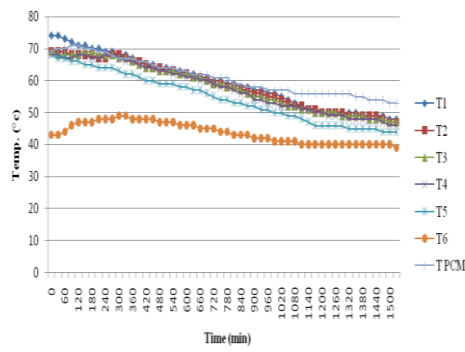


Fig. 24. Discharging with Spiral PCM Module.

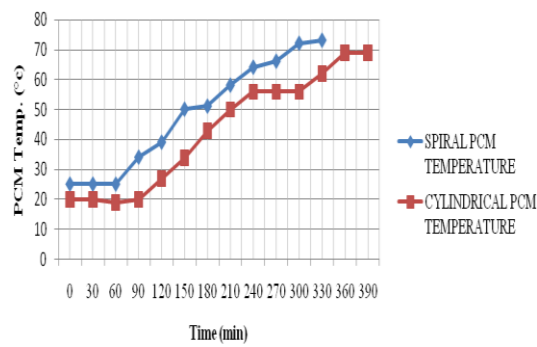


Fig. 25. Comparison of PCM Temperature (Charging).

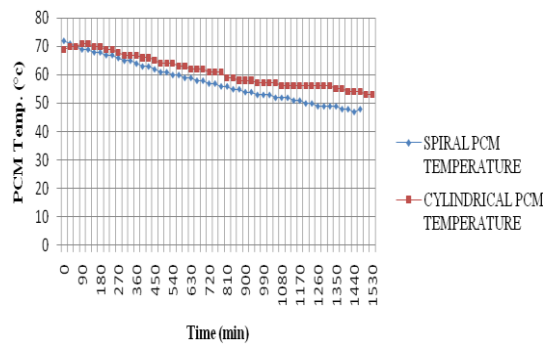


Fig. 26. Comparison of PCM Temperature (Discharging).

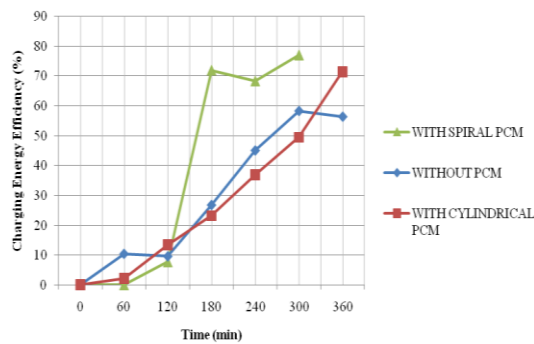


Fig. 27. Comparison of Charging Energy Efficiency.

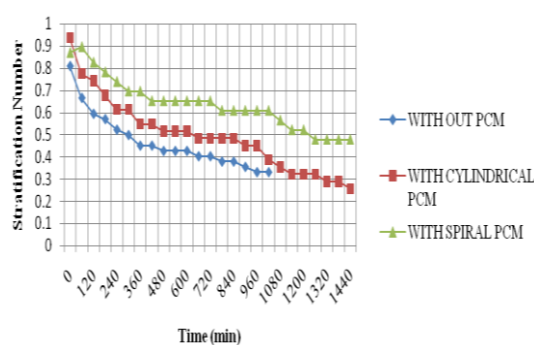


Fig. 28. Comparison of Stratification Number.

During the charging period, the measurements was done until an average temperature of  $65^{\circ}\text{C}$  is reached inside the solar tank with and without PCM modules. From this experiment, it was observed that when spiral PCM modules used, higher charging energy efficiency is obtained. The main reason is due to higher heat transfer rate and large surface area in spiral PCM module. It took 6.30 hours for charging without PCM and the same in the case of cylindrical PCM module. But it took only 5:30 hours in the case of spiral PCM module. During the discharging period, the measurements were done until an average temperature of  $45^{\circ}\text{C}$  is reached. For without PCM module, it took about 19 hours to discharge and in the case of cylindrical PCM module and spiral PCM module, it took about 25 hours and 24 hours respectively. Hence, it is clear that cylindrical and spiral PCM modules have some high discharging time period.

## 5. Conclusions

Transition metal chalcogenides have gained worldwide attention in recent decades and are being researched for use in different applications due to their unique properties. In this present study, the XRD, Raman spectroscopic and DSC analysis were performed to study the thermal properties of the transition metal chalcogenide/graphene samples. The thermo-electric properties of chalcogenide materials possess excellent thermal stability. The Transition Metal Chalcogenide have higher thermal stability and graphene have a higher thermal conductivity. The imperative properties of graphene and TMC is added to form the PCM for increasing the material stability and conductivity.

Energy storage in PCM has a lot of advantages over sensible systems because of the lower mass and volume of the system. In this present study, the theoretical and experimental validation was performed with charging and discharging of PCM with spiral module and these results are compared with cylindrical PCM module. The result shows a drastic change in charging and discharging time period when compared with and without PCM. Moreover, extensive study is required to meet the design challenges and the requirement of the future energy storage and conversion.

## References

- [1] F. Bonaccorso, L. Colombo, G. Yu, M. Stoller, V. Tozzini, A C. Ferrari, Science **347**(6217), 1246501 (2015).
- [2] Xiaogan Li Ding Gu, Tin Oxide Materials Synthesis, Properties, and Applications, 281 020).
- [3] ZhenghuaTang, HongyuYang, Micro and Nano Technologies, 355 (2020).
- [4] H. Yuan, L. Kong, T. Li, Q. Zhang, Chinese Chemical Letters **28**(12), 2180 (2017).

- [5] A. Kagkoura, T. Skaltsas, N. Tagmatarchis, *Chemistry A European Journal* **23**(53), 12967 (2017).
- [6] M. K. Jana, C. N. R. Rao *Phil. Trans. R. Soc. A.* **374**, 0318 (2016).
- [7] R. Jain, R. Narayan, S. P. Sasikala, K. E. Lee, H. J. Jung, S. O. Kim, *2D Materials* **4**(04), 2006 (2017).
- [8] T. Heine, *Accounts of Chemical Research* **48**(1), 65 (2015).
- [9] Q. H. Wang, K. K. Zadeh, A. Kis, J. N. Coleman, M. S. Strano, *Nature Nanotechnology* **7**, 699 (2012).
- [10] L. Arulmurugan, M. Ilangkumaran, *Journal of Ovonic Research* **13**(6), 299 (2017).
- [11] A. H. Castro Neto, F. Guinea, N. M. R. Peres, K. S. Novoselov, A. K. Geim, *Rev. Mod. Phys.* **81**, 109 (2009).
- [12] A. K. Geim, *Science* **324**, 1530 (2009).
- [13] A. A. Balandin, *Nano Letters* **8**, 902 (2008).
- [14] A. S. Mayorov, *Nano Letters* **11**, 2396 (2011).
- [15] L. F. Mattheis, *Physics Review B* **8**, 3719 (1973).
- [16] J. A. Wilson, A. D. Yoffe, *Advanced Physics* **18**, 193 (1969).
- [17] A. Ayari, E. Cobas, O. Ogundadegbe, M. S. Fuhrer, *Journal of Applied Physics* **101**, 014507 (2007).
- [18] T. Lu, S. Dong, C. Zhang, L. Zhang, G. Cui, *Coordination Chemistry Reviews* **332**(1), 75 (2017).
- [19] W. Choi, N. Choudhary, G. H. Han, J. Park, D. Akinwande, Y. H. Lee, *Materials Today* **20**(3), 116 (2017).
- [20] V. Gowtham, L. Arulmurugan, *International Journal of Scientific Engineering and Technology Research* **3**, 712 (2014).